Anomalous energy dissipation in molecular-dynamics simulations of grains: The "detachment" effect

S. Luding,[1,*] E. Clément,[2] A. Blumen,[1] J. Rajchenbach,[2] and J. Duran[2]
[1]*Theoretische Polymerphysik, Universität Freiburg, Rheinstraße 12, D-79104 Freiburg, Germany*
[2]*Laboratoire d'Acoustique et d'Optique de la Matière Condensée, Université Pierre et Marie Curie 4, place Jussieu, 75005 Paris, France*
(Received 9 February 1994)

We study models for granular materials using both molecular-dynamics (MD) and event-driven (ED) methods. In the MD simulations we implement linear as well as nonlinear interaction laws. In the case of multiparticle interactions, we find that MD calculations lead to an anomalous energy loss. In this paper we elucidate this effect and the conditions under which it appears.

PACS number(s): 46.10.+z, 05.60.+w, 05.40.+j

I. INTRODUCTION

Nature offers numerous examples for noncohesive granular materials such as sand or pebbles. Also in the industrial world powder processing is of crucial interest. The phenomenological behavior of such systems, halfway between solids and liquids, is full of surprises [1]; up to now the basic physics is not well understood [2]. In particular, a vibrated powder exhibits properties that resemble a fluid such as convection rolls [3–5] and surface fluidization [6–8] but sometimes with peculiar behaviors such as heaping [4–6], size segregation [9–11], bulk dilatation [12–14], and also surprising propagation properties of the sound waves [15]. Analytical approaches to the problem of granular materials are, for example, Refs. [16–20].

Recently, experimental evidence of spontaneous convection rolls was reported on three-dimensional (3D) granular materials [4,5] as well as 2D model media [7]. In parallel, experiments have motivated a great deal of computer work, since numerical simulation is an important complementary tool which accesses physical quantities which are almost impossible to get directly from experiments, such as energy transfer, microfluctuations, or vault effects. Thus it is crucial to develop reliable computer algorithms that can, at least, reproduce correctly the macroscopic phenomenology.

At the moment, a majority of simulations use molecular-dynamics techniques [21] which involve *ad hoc* microscopic assumptions such as linear spring-dashpot interaction laws [22–28], nonlinear interaction laws, and static as well as dynamic friction [29–32]. In another group are simulation calculations which follow series of binary collisions for assemblies of hard spheres [33–40]. Simulations based on binary collisions are hampered by the fact that for a certain threshold of energy loss, the collision frequency between the beads is bound to diverge and clusters will form. Thus a prescription has to be elaborated to handle the possibility of having connected clusters [38,39].

Recently, two independent groups of authors [25,27] have reported, based on molecular-dynamics (MD) simulations, spontaneous convection in vibrated granular models. The calculations are related to effects found experimentally in hard-sphere systems. Thus the question arises as to how far MD methods faithfully reproduce hard-sphere collisions, especially in situations in which the systems are made up of many particles. As we proceed to show, MD calculations produce spurious effects, which may be responsible for the appearance of convection patterns.

Here we investigate an assembly of beads which interact with each other. At first we introduce the different simulation methods: molecular-dynamics and also hard-sphere-type methods. We discuss the choice of the forces used in the simulations and we relate the internal MD parameters to the momentum restitution coefficient; the last quantity is of utmost importance in calculations which focus on collisions of hard spheres. Then we show on a simple 1D toy model that in MD simulations an anomalous behavior appears, connected to large fluctuations in the distances between beads, in their energy loss and in the dilatancy threshold (connection to collective motion). This behavior is due to the MD model forces acting on the beads and may subsist even in the limit of very hard interactions. We call this behavior "detachment effect," because under certain conditions the particles separate completely. This effect is different from the so-called decompaction which was evidenced in 2D dissipative granular systems [41]. The effect there was due to the friction with the walls and not due to the elastic properties of the material. Furthermore, we show that the detachment effect is amplified for larger numbers of beads and longer contact times. We present a comparison of ED and MD simulations and relate these to experimental results. We also give arguments that the detachment effect may lead in 2D to the appearance in the MD calculations of convection rolls [42]; this means that convection may disappear when the interactions used in the calculations are rendered "hard," as is necessary to model, say, steel beads.

*Electronic address: lui@tpoly2.physik.uni-freiburg.de

II. THE SIMULATION METHODS

In common experience, hard beads have rather well-defined binary collision properties [40]. In general, one defines for each type of material a momentum restitution coefficient which is found to be weakly dependent on velocity in the experimentally accessible velocity range around 1 m/s. It is therefore a natural idea to use this property to monitor the collision sequence of an assembly of beads in an event-driven (ED) way. Furthermore, as we show in the next section, this coefficient has a counterpart in a MD model with linear interactions and thus it allows a direct comparison between the ED and the MD methods.

A. MD simulations

In the MD simulations we follow the dynamics of a system of N spherical particles with diameters d_i ($i=1,\ldots,N$). d_i equals d_0 for simulations with equal radii, or d_i is chosen randomly from a homogeneous distribution of width w. In the 1D simulations the particles are placed on a vertical line (thus only the lowest particle interacts with the bottom plate); in the 2D simulations the particles are put in a container of width L and infinite height; here one may use either periodic boundary conditions or horizontally fixed walls. The bottom plate in 1D, or the container in 2D may carry out a sinusoidal motion:

$$z_0(t)=A_0\sin(2\pi ft)\ . \tag{1}$$

In the MD calculation a fifth-order predictor-corrector algorithm is used [27]. Two particles (or a particle and a wall) interact when their relative distance $r_{ij}=|\mathbf{r}_{ij}|$ (where $\mathbf{r}_{ij}$ points from the center of i to the center of j) is smaller than the sum of their radii (the radius of the particle). In this regime, $d_i+d_j>2r_{ij}$, three forces are active. First, an elastic restoration force

$$\mathbf{f}_{\rm el}^{(i)}=-K[\tfrac{1}{2}(d_i+d_j)-r_{ij}]\mathbf{n}_{ij}\ , \tag{2}$$

where $\mathbf{n}_{ij}=\mathbf{r}_{ij}/r_{ij}$ is the normal direction of contact and K is the spring constant. Second, a frictional force in the normal direction,

$$\mathbf{f}_n^{(i)}=-D_n m_{ij}[\mathbf{v}_{ij}\cdot\mathbf{n}_{ij}]\mathbf{n}_{ij}\ , \tag{3}$$

where $\mathbf{v}_{ij}$ is the relative velocity of particles i and j, D_n is the normal dissipation parameter, and m_{ij} is twice the reduced mass of particles i and j, $m_{ij}=2m_im_j/(m_i+m_j)$. Third, a frictional force in the tangential direction,

$$\mathbf{f}_t^{(i)}=-D_t m_i[\mathbf{v}_{ij}\cdot\mathbf{t}_{ij}]\mathbf{t}_{ij}\ , \tag{4}$$

where $\mathbf{t}_{ij}=(-n_{ij}^y,n_{ij}^x)$ is the vector $\mathbf{n}_{ij}$ rotated by 90° and D_t is the tangential dissipation parameter. In our simulations we include the forces Eqs. (2) and (3) in 1D and Eqs. (2)–(4) in 2D; however, we neglect the rotation of the particles and also the static friction.

B. Event-driven simulations in 1D

In a recent work [39] numerous simulations were carried out for a 1D column of particles. For those simulations an ED algorithm was used. Event-driven simulations consist in monitoring a sequence of events (i.e., collisions) between which Newton's equations of motion for each particle are solved exactly. For particles, an event is defined either by a sudden change in momentum (collision) or by the take off from the bottom plate. In the following, for 1D simulations, the N beads are numbered from below starting with $i=1$; for the bottom plate we set $i=0$. Between events each particle i follows its own trajectory; this is so, because we assume dissipation to occur only on collision. For events occurring at distinct times the sequence of collisions is well defined by their sequence in time. For events which happen simultaneously the collisions get ordered following the largest relative velocity (LRV) procedure [38,39]: The procedure consists in sequentially picking up the pair of particles with the largest relative velocity $v_{i-1}-v_i$, letting them collide, and then updating the respective velocities. The procedure stops when all relative velocities are smaller than a certain threshold. For an extended description of LRV see Refs. [38,39]. We stop to note that there is a fundamental difference between MD simulations, where the duration of a collision (i.e., the time t_c the beads are in contact) is larger than zero and ED algorithms where one has $t_c=0$.

III. MODELS USED IN SIMULATIONS

A. The spring-dashpot model

Usually MD simulations of powders are based on the linear spring-dashpot model (LSD) [23–26]. Here the penetration x along the line connecting the centers of the particles obeys the linear differential equation

$$\ddot{x}+2\mu\dot{x}+\omega_0^2x=0\ , \tag{5}$$

where the parameters μ and ω_0 are adjustable. In terms of the reduced mass $m=m_1m_2/(m_1+m_2)$, of the dashpot loss coefficients D_n and D_t, and of the spring constant K one has $\omega_0=\sqrt{K/m}$, and $\mu=D_n$ for central collisions of two particles ($\mu=D_n/2$ for the perpendicular collision of one particle with a wall). For two colliding particles the contact time is

$$t_c=\pi/\sqrt{\omega_0^2-\mu^2}\ , \tag{6}$$

a quantity independent of the initial relative velocity v_0 [23–25]. From t_c one obtains the coefficient of restitution ε as being

$$\varepsilon=-\dot{x}(t_c)/v_0=e^{-\mu t_c}=e^{-\mu\pi/\sqrt{\omega_0^2-\mu^2}}\ . \tag{7}$$

Note that here ε is also independent of v_0. For low dissipation the maximal penetration is $x_{\max}=v_0/\omega_0$.

The coefficient of restitution ε is known from experiments [43] for collision velocities v_0 around 1 m/s. Here we observe that there are many choices for μ and ω_0, which lead via Eq. (7) to the same ε; these choices, however, lead to different t_c values. It is therefore important to discuss which of these t_c values are realistic. This leads us to consider also nonlinear interaction models.

As we recall, for two colliding spheres t_c can be evaluated using an expression which goes back to Hertz [44]. For steel beads of diameter $d=1.5$ mm, one obtains for velocities of 1 m/s a value of $t_c \approx 4.6\times10^{-6}$ s (see below). Hence for time-driven MD simulations one has to use time steps at least one order of magnitude smaller than t_c. Hence, to simulate one second, some 10^7 steps are needed, which means a lot of computer power.

B. Nonlinear interaction models

Linear interactions are not an accurate description for rigid bodies, since the surface of contact generally depends on the compression. On phenomenological grounds we consider the following general compression-dissipation equation:

$$m\ddot{x}+\eta d\left[\frac{x}{d}\right]^{\gamma}\dot{x}+Ed\left[\frac{x}{d}\right]^{\beta}x=0\ . \tag{8}$$

Here E and η are material and shape dependent; E depends on the Young modulus and the Poisson ratio, and η depends on both the shearing and compression viscosities. Note that the loss channel in Eq. (8) is only viscoelastic; thus neither a plastic permanent deformation nor a loss due to residual vibrations stored in the spheres after collision are included. Furthermore, the nonlinear terms are formulated as functions of (x/d), where d is the diameter of the beads, in order to keep the structure of the equation close to that of Eq. (5). As we proceed to show, several models used in literature are special cases of Eq. (8). The simplest form ($\beta=\gamma=0$) leads to Eq. (5). For two spheres Hertz calculated the elastic interaction parameter E due to a symmetric deformation; this leads to $\beta=\frac{1}{2}$ [44]. Different recent works used this interaction law [28,29] together with a linear loss coefficient ($\gamma=0$). Kuwabara and Kono [43] generalized the Hertz argument to deal with viscoelastic loss; they obtain $\gamma=\frac{1}{2}$. Taguchi [45] extended the expression by including also a nonlinear dependence of the dissipation on the velocity. In the Appendix we present scaling arguments which allow us to estimate from Eq. (8), in the limit of low dissipation, the dependence of the momentum restitution coefficient ε on the initial velocity v_0.

Equation (A2) of the Appendix, with $\beta=\frac{1}{2}$ and $\gamma=0$, reproduces Hertz's equation. One has $E=Y/[3(1-\bar{\sigma}^2)]$ where Y is the Young modulus and $\bar{\sigma}$ is the Poisson ratio. We calculate the order of magnitude of t_c for steel beads of diameter $d=1.5$ mm. For steel we use $Y=2.06\times10^{11}$ N/m^2, $\bar{\sigma}=0.28$, and $m=1.38\times10^{-5}$ kg and obtain for an initial velocity of 1 m/s a contact time of $t_c\approx4.6\times10^{-6}$ s, when dissipation is ignored, i.e., the result mentioned above; for aluminum, for which one has $Y=0.71\times10^{11}$ N/m^2, $\bar{\sigma}=0.34$, and $m=0.479\times10^{-5}$ kg one again obtains a contact time t_c of around 4.6×10^{-6} s. The estimate is less precise here because of the large dissipation of aluminum beads. We note that Hertz's expression, valid for low dissipation, shows a weak dependence of t_c on the velocity, i.e., $t_c \propto v_0^{-1/5}$.

Furthermore, we stress the fact that once a reasonable t_c value is chosen, one can model the dynamics using even simple LSD interactions. This is the idea behind a large number of works on the problem. In the following, we shall use mainly the simple LSD interaction laws. Choosing a pair of values for ε and t_c appropriate to the material fixes the parameters μ and ω_0 in Eq. (5) unambiguously. Thus for spheres made of steel $\varepsilon=0.9$; for spheres with diameter $d=1.5$ mm we use $t_c=4.6\times10^{-6}$ s which leads to $\omega_0\approx6.8\times10^5$ s^{-1} and to $\mu\approx2.3\times10^4$ s^{-1}. For aluminum $\varepsilon=0.6$ so that using $t_c\approx4.6\times10^{-6}$ s one has roughly $\omega_0\approx6.8\times10^5$ s^{-1} and $\mu\approx1.1\times10^5$ s^{-1}. These values for ω_0 and μ are much larger than what has been commonly used in former simulation approaches and lead, for an initial velocity $v_0=1$ m/s, to a penetration depth of $x_{\max}\approx1.5\times10^{-6}$ m, which means 0.1% of the diameter. Other simulations [25,27] (both have a different size and time scaling) use ω_0 and μ values which lead to a penetration depth of a few percent of the particle's diameter for particle velocities in the order of magnitude of the maximum velocity of the vibrating box $v_0\cong A_0\omega$. Note here again, that taking a very low value for t_c requires involved computing power. The problem is really to know whether it is of much importance to use such low contact times. This is the question we address in the following.

IV. THE DETACHMENT EFFECT

Now we are interested in probing the collective behavior of an array of beads in a simple one-dimensional toy-model. In this subsection we neglect gravity effects and focus on the collision of this array of beads with a static boundary. This situation is interesting since it allows us to compare MD results with those obtained using the ED algorithms [33,35,36,38,39]. In Figs. 1(a)–1(c) we plot the results of MD simulations for $N=10$, $\varepsilon=0.9$, $v_0=-0.2$ m/s, and $t_c=0.7\times10^{-5}$ s. The y axis displays the reduced height

$$z_i=h_i-(N-1)d-d/2\ , \tag{9}$$

where h_i is the height of the center of bead i. The values μ and ω_0 are then obtained using Eqs. (6) and (7); further on they fix via $K=m\omega_0^2$ and $D_n=\mu$ the parameters to be used for binary collisions. In Fig. 1(a) we start from an initial separation between neighboring particles of $s_0=0$ m; in Fig. 1(b) we use $s_0=10^{-6}$ m and in Fig. 1(c) we use $s_0=10^{-5}$ m. In Figs. 1(d)–1(f) we plot the results of ED simulations with $N=10$, $\varepsilon=0.9$, and $v_0=-0.2$ m/s; we again use $s_0=0$ m [Fig. 1(d)], $s_0=10^{-6}$ m [Fig. 1(e)], and $s_0=10^{-5}$ m [Figs. 1(f)]. For ED simulations the contact time t_c is zero. Comparing Figs. 1(a) and 1(b) with 1(d) and 1(e), respectively, shows that the outcome of MD simulations differs from the one for ED in the case of very small initial separations; the final velocity of the particles' center of mass (c.m.) turns out to be larger in MD simulations; furthermore, the interparticle separations after the collisions are relatively ordered for ED and quite disordered for MD simulations. Evidently this finding may be a means to check experimentally the computational methods. On the other hand, for sufficiently large initial separations [see Figs. 1(c) and 1(f)] MD and

ED simulations lead to qualitatively similar results. We furthermore note that the ED procedures lead both for $s_0 > 0$ and also for $s_0 = 0$ to similar results; the situation is different for MD. To be more quantitative we now introduce the effective restitution coefficient through $\varepsilon_{\text{eff}} = \sqrt{E_f / E_0}$, where E_0 and E_f denote the initial and final energies. We furthermore define the *relative* kinetic energy (also called "granular temperature" [17]) through $E_r = \frac{1}{2}\sum_{i=1}^{N} m_i (v_i - v_{\text{c.m.}})^2$; E_r is also a measure of the typical separation of the beads after rebound. In Fig. 2(a) we plot ε_{eff} obtained from MD simulations as a function of the initial separation s_0; we rescale the axes in such a way that the ratio of the external time between contacts s_0/v_0 to the internal contact time t_c shows up, i.e., we set $\sigma = s_0/v_0 t_c$.

In Fig. 2 we have $N = 10$, $d = 1$ mm, and $\varepsilon = 0.9$. The initial velocity v_0 is varied between 14 and 0.008 m/s; t_c is varied between 2.2×10^{-3} and 2.5×10^{-6} s. For each pair (v_0, t_c), s_0 is varied between 10^{-9} and 10^{-3} m. In Fig. 2(a) we plot ε_{eff} as a function of σ. We find that all

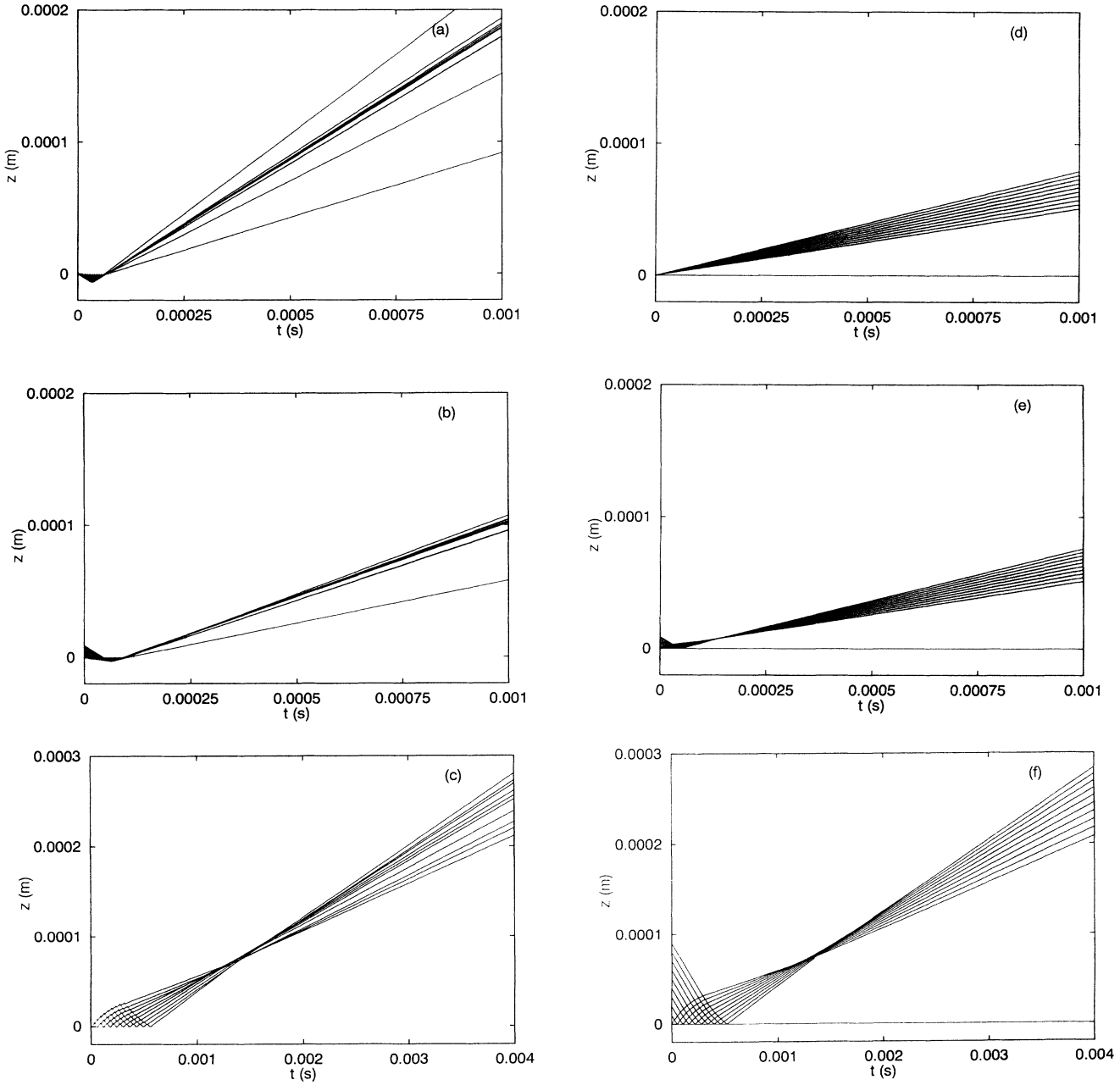

FIG. 1. (a) MD trajectories of the centers of $N = 10$ particles which collide with a fixed boundary. Here $\varepsilon = 0.9$, $t_c = 0.7 \times 10^{-5}$ s, $v_0 = -0.2$ m/s, and $s_0 = 0$ m. The positions are in reduced units, Eq. (9). (b) The same as in (a) but with $s_0 = 10^{-6}$ m. (c) The same as in (a) but with $s_0 = 10^{-5}$ m. Note the different axes. (d) ED trajectories of the centers of $N = 10$ particles; the parameters are as in (a); especially $s_0 = 0$ m. (e) The same as in (d) but with $s_0 = 10^{-6}$ m. (f) The same as in (d) but with $s_0 = 10^{-5}$ m. Note the different axes.

results scale; they lie on a universal curve which depends only on σ. We also mention that a simulation with random initial separation (i.e., each particle i at position $z_i = is_0$ is shifted by a random value taken from the interval between $-s_0/2$ and $s_0/2$) also falls on the same curve. Two features are prominent: first, when $\sigma \ll 1$ the energy loss is very small. This leads to large fluctuations in the interparticle distances after the collision with the plate, a phenomenon which we call detachment effect. Second, for $\sigma \gg 1$ the MD solution gets near to the ED result and the energy loss gets to be only slowly dependent on σ [right side of Fig. 2(a)]. The ED procedure leads for various s_0 values ($s_0 = 0$, 10^{-7}, 10^{-6}, 10^{-5}, 10^{-4}, 10^{-3}, and 10^{-2} m), $N = 10$, and $\varepsilon = 0.9$ to $\varepsilon_{\text{eff}} \cong 0.341 \pm 0.002$ [the dashed line in Fig. 2(a)]. We varied v_0 between 20 and 0.01 m/s. As a general remark, we note that the ED procedure [38,39] leads to practically s_0- and v_0-independent ε_{eff}, and we find that ε_{eff} is considerably smaller than ε.

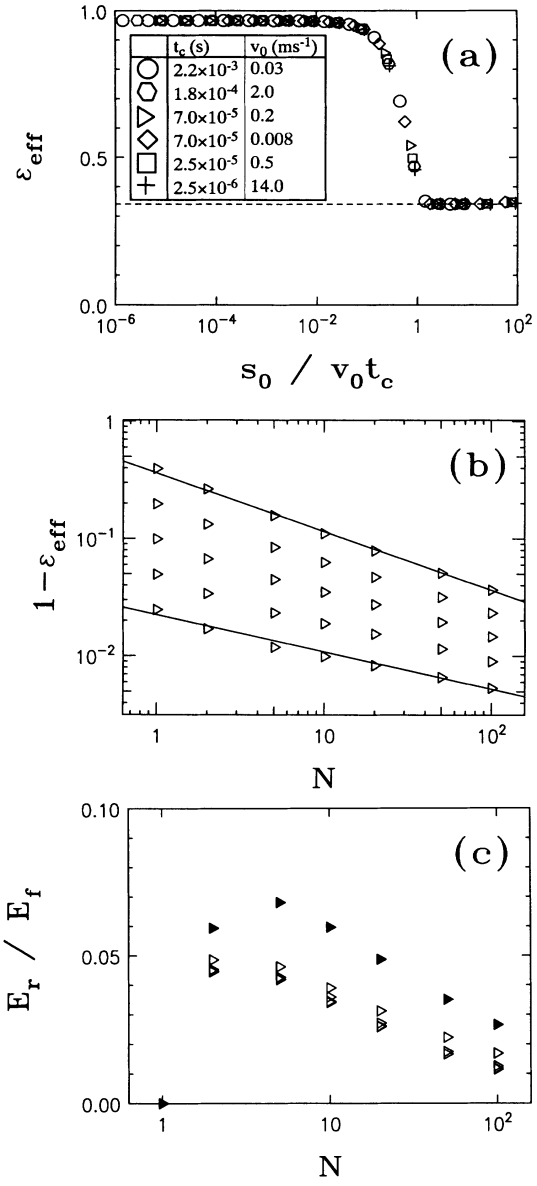

FIG. 2. (a) Linear-logarithmic plot of the effective restitution coefficient ε_{eff} as a function of $\sigma = s_0/v_0 t_c$. Here the MD calculation involved $N = 10$ particles colliding with a fixed boundary. We have $\varepsilon = 0.9$ and $d = 1$ mm, while v_0 and t_c are given in the inset. The dashed line indicates the result of the LRV procedure. (b) Log-log plot of $1 - \varepsilon_{\text{eff}}$ as a function of N for $s_0 = 0$, $v_0 = 0.05$ m/s, and $t_c = 0.2 \times 10^{-4}$ s. Here N varies from 1, 2, 5, 10, 20, 50, to 100 and ε varies from 0.6, 0.8, 0.9, 0.95 to 0.975 from top to bottom for each N value. The dashed lines indicate the slopes -0.5 (top) and -0.315 (bottom). (c) Plot of E_r/E_f as a function of N (E_r: relative kinetic energy after collision; E_f: total kinetic energy after collision). The parameters are as in (b). The filled triangles correspond to $\varepsilon = 0.6$.

A. The energy loss during collisions

We now analyze for MD the case of a colliding column with zero initial separation (cluster) and look into the energy loss as a function of both internal (ε, t_c) and also external (v_0, N) parameters. In Figs. 2(b) and 2(c) we set $s_0 = 0$, $v_0 = 0.2$ m/s, and $t_c = 0.2 \times 10^{-4}$ s and vary N and ε. In Fig. 2(b) we plot on double-logarithmic scales the effective dissipation $1 - \varepsilon_{\text{eff}}$ as a function of N for different ε; we find that $1 - \varepsilon_{\text{eff}}$ depends nonlinearly on the number of particles and that the energy loss *decreases* with increasing N. This is a rather surprising feature. In Fig. 2(c) we plot the E_r/E_f where E_r is the relative energy and E_f is the total energy after collision. The simulations are the same as in Fig. 2(b). For $N = 10$ and $\varepsilon = 0.9$ we find, as an example, E_r/E_f to be 0.035. This means that after the collision the particles separate; we have detachment.

We have determined from simulations for $s_0 = 0$ the total time of the interaction, t_k, of the whole column of beads with the wall. We find that t_k is *proportional* to the number of beads and to the contact time; hence $t_k \approx N t_c$. This is consistent with viewing the beads as a series of elastic springs. We furthermore find that $E_r \propto v_0^2$; by varying ε in the limit of low dissipation, $\varepsilon > 0.9$, we find that $\varepsilon_{\text{eff}} \propto \varepsilon$. Thus the "detachment effect" is the result of model-dependent dissipation properties. Inside the column the energy is dissipated mainly in interactions involving particles with high relative velocities. Since during the collision with the wall the column of beads gets compressed, the energy is dissipated preferentially between beads at the boundary of the compressed and the relaxed region. Keeping the other parameters fixed, the size of the boundary area depends only weakly on N (this leads to the nonlinear dependence on N). Even in the case of very high dissipation (i.e., $N = 10$ and $\varepsilon = 0.6$) detachment occurs, while ED simulations with the LRV procedure lead to an ε_{eff} which practically vanishes, i.e., to a clustered column.

B. The dependence of the detachment effect on the interaction law

We carried out a series of simulations in 1D for different interaction laws and different numbers N of particles which hit the wall. The nonlinear elastic force is, as an extension of Eq. (2),

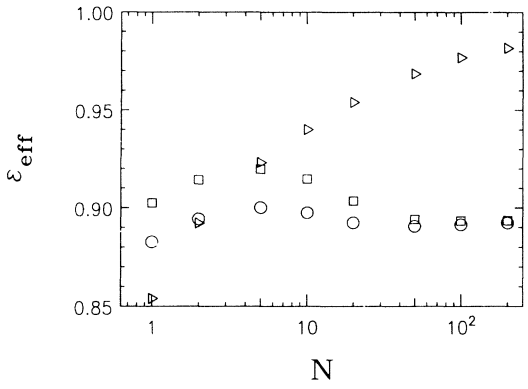

FIG. 3. The effective restitution coefficient ε_{eff} plotted as a function of N for $s_0=0$, $v_0=0.05$ m/s. Here N varies from 1, 2, 5, 10, 20, 50, 100 to 200. We used the Hooke interaction ($\beta=\gamma=0$, triangles), the Hertz interaction ($\beta=\frac{1}{2}$, $\gamma=0$, squares), and the Hertz-Kuwabara interaction ($\beta=\gamma=\frac{1}{2}$, circles). See text for details.

$$\mathbf{f}_{el}^{(i)}=-K[\tfrac{1}{2}(d_i+d_j)-r_{ij}]^{1+\beta}\mathbf{n}_{ij}$$

and the nonlinear dissipative force is an extension of Eq. (3),

$$\mathbf{f}_{n}^{(i)}=-D_n m_{ij}[\mathbf{v}_{ij}\cdot\mathbf{n}_{ij}][\tfrac{1}{2}(d_i+d_j)-r_{ij}]^{\gamma}\mathbf{n}_{ij}\ ,$$

where $r_{ij}<(d_i+d_j)/2$.

In Fig. 3 we plot the effective restitution coefficient as a function of N for $s_0=0$, $v_0=0.05$ m/s, $d=1$ mm, and for different interaction laws. Using the linear interaction law with $\beta=\gamma=0$, $K/m=2\times10^9$ s^{-2}, and $D_n=3.17\times10^3$ s^{-1} we find that ε_{eff} increases with N. Using the Hertz-type interaction with $\beta=\frac{1}{2}$, $\gamma=0$, $K/m=2\times10^{12}$ s^{-2}m$^{-1/2}$, and $D_n=2\times10^3$ s^{-1} or a more general form with $\beta=\gamma=\frac{1}{2}$, $K/m=2\times10^{12}$ s^{-2}m$^{-1/2}$, and $D_n=10^5$ s^{-1}m$^{-1/2}$ we find that ε_{eff} varies little as a function of N. The net result is that the detachment effect is weaker for nonlinear interactions; nonetheless there is still a fundamental difference to ED algorithms, for which ε_{eff} is close to zero for $N(1-\varepsilon)$ large [39].

C. The detachment effect in 2D

Paralleling the 1D MD simulations we perform 2D calculations on a system of particles which hit a wall. The initial velocity v_0 is taken to be the same for all particles. At start we put all particles on a periodic, triangular, lattice with lattice constant $a=d+s_0$, width of $L=13a$, and height $h=N/13$ lattice points. Then we introduce randomness by shifting each particle horizontally and vertically by a random amount between $-s_0/2$ and $s_0/2$ (here we took care that no overlap exists in the initial configuration). Then we let this system hit the wall and after the collision we determine again ε_{eff}. Here the process is considered to be finished, when in a time interval of $2Ns_0/v_0$ no collision occurs (i.e., no contact exists).

In Fig. 4(a) we plot the effective restitution coefficient ε_{eff} as a function of $\sigma=s_0/v_0t_c$ for $N=130$ particles with $d=1$ mm which collide with a wall. Here $\varepsilon=0.9$ and s_0 varies between 10^{-7} and 10^{-3} m, v_0 varies between 1 and 0.01 m/s, and t_c varies between 10^{-4} and 0.2×10^{-5} s. The transition from the dissipative regime (large σ) to the detachment regime (small σ) is less sharp in 2D (the transition takes place in the interval $0.1<\sigma<10$), than in 1D (the transition takes place in the interval $0.1<\sigma<1$). Note that in both limits (small or large σ) ε_{eff} does not depend on the dimensionality, but only on the height $L=Na/L$ and on ε (in 1D $L/a=1$). This is also obvious from Fig. 4(b), where we plot the effective dissipation $1-\varepsilon_{eff}$ as a function of h for vanishing initial separation s_0. We use $\varepsilon=0.6$ (circles) and $\varepsilon=0.9$ (triangles) and compare the data of 2D with the results of 1D (crosses), already displayed in Fig. 2(b). From this figure we infer that arrays of particles with equal height behave similarly in 1D and in 2D, as long as the particle separation is small.

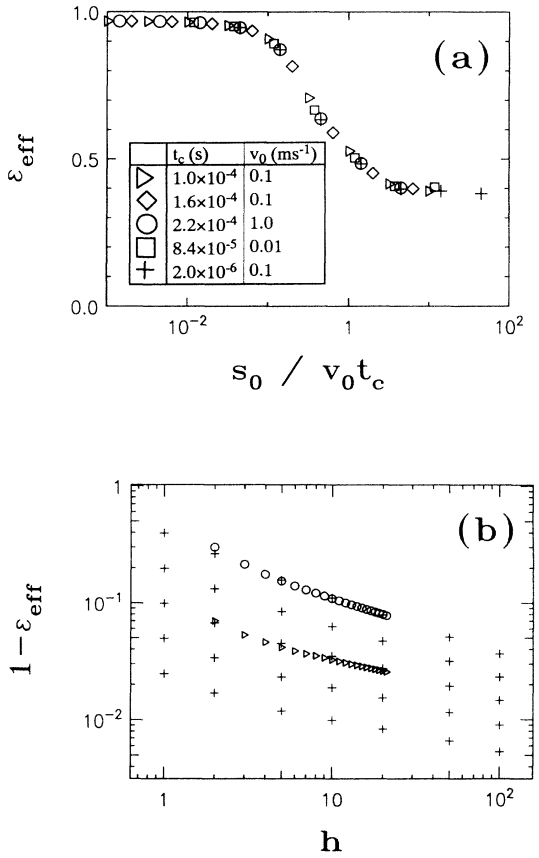

FIG. 4. (a) Linear-logarithmic plot of the effective restitution coefficient ε_{eff} in two dimensions, as a function of $\sigma=s_0/v_0t_c$. The parameters are $\varepsilon=0.9$, $N=130$, and $d=1$ mm; v_0 and t_c are given in the inset. (b) Log-log plot of the effective dissipation $1-\varepsilon_{eff}$ as a function of h for $s_0=0$, $v_0=0.05$ m/s, and $t_c=0.2\times10^{-4}$ s. The height h varies in steps of one from $h=2$ to 21 for $\varepsilon=0.9$ (triangles) and for $\varepsilon=0.6$ (circles). The crosses display the 1D data of Fig. 2(b).

V. COMPARISON OF ED AND MD SIMULATIONS WITH THE EXPERIMENT

In this section we investigate the behavior of a column of beads undergoing vibrations in a gravity field. For this we let the bottom plate vibrate according to Eq. (1). The aim of this section is to find out under which conditions MD and ED results are comparable and when deviations in the computed macroscopic properties occur. We also present experimental results; these are better reproduced by ED than by MD simulations.

A. The anomalous behavior of an excited column of beads

In Fig. 5 we present the MD trajectories of the centers of the beads calculated using $N=10$ and $\varepsilon=0.6$. The bottom plate moves according to Eq. (1) with amplitude $A_0=1.24d$ and frequency $f=20$ Hz; this leads to a maximal acceleration of $2g$ (where g is the gravitational acceleration). The y axis displays the reduced height $z_i=h_i-(N-1)d-d/2$, where h_i is the height of the center of bead i. The value $\varepsilon\cong 0.6$ is typical for aluminum beads. From previous studies we know, both from experiments and from ED simulations [38,39], that such a collection of beads ($N=10$, $\varepsilon=0.6$ has a very low effective restitution coefficient ($\varepsilon_{\text{eff}}\cong 0$) and that the system forms a cluster whose behavior mirrors that of a very inelastic single bead [46]. The MD results were obtained for $t_c=0.7\times 10^{-3}$ s [Fig. 5(a)] and $t_c=0.7\times 10^{-5}$ s [Fig. 5(b)]. Note that there occur large fluctuations in the interbead separations; this is due to the fact that the contact time of ten particles with the bottom plate is roughly 15% of the period and is thus too large to decouple the collisions from the vibration. In Fig. 5(b), where the contact time of the beads is much shorter than the excitation period, we observe a pattern which alternates between condensed states, with almost zero relative energy, and states with large interbead separations due to large relative energies. In the condensed state we find very small separations; thus $\sigma=s_0/v_0t_c\ll 1$ is very small and therefore the detachment effect is active (which means that the next collision sequence occurs under very low-energy loss). After this collision sequence the separations between beads get to be large, i.e., $\sigma>1$. Therefore in the next collision sequence much energy is lost, so that the separations again decrease. This periodic change from high to low σ values and back again is the reason for the pattern observed in Fig. 5(b). On the other hand, for high t_c values σ stays small most of the time so that the system remains in a high-energy state, in which detachment occurs.

An ED algorithm as introduced in Refs. [38,39] shows a totally different behavior in this parameter range. For $N=10$ and $\varepsilon=0.6$ the event-driven LRV procedure leads to $\varepsilon_{\text{eff}}\approx 0$ (the *inelastic collapse* [33–36]); in other words, the energy of collision is always dissipated inside the column, so that the particles stay clustered. This leads to a pattern for the c.m. trajectory similar to the one of a single, totally inelastic particle [46].

B. Comparison with experiments

Now we present two experiments for a collection of aluminum beads which are moved vertically. The result is that in 1D the beads behave more or less as a cluster; if microfluctuations in the positions exist, they occur at a scale much smaller than the size of the beads.

We investigate a vertical column of aluminum beads. The diameter of the beads is $d=3$ mm. A description of

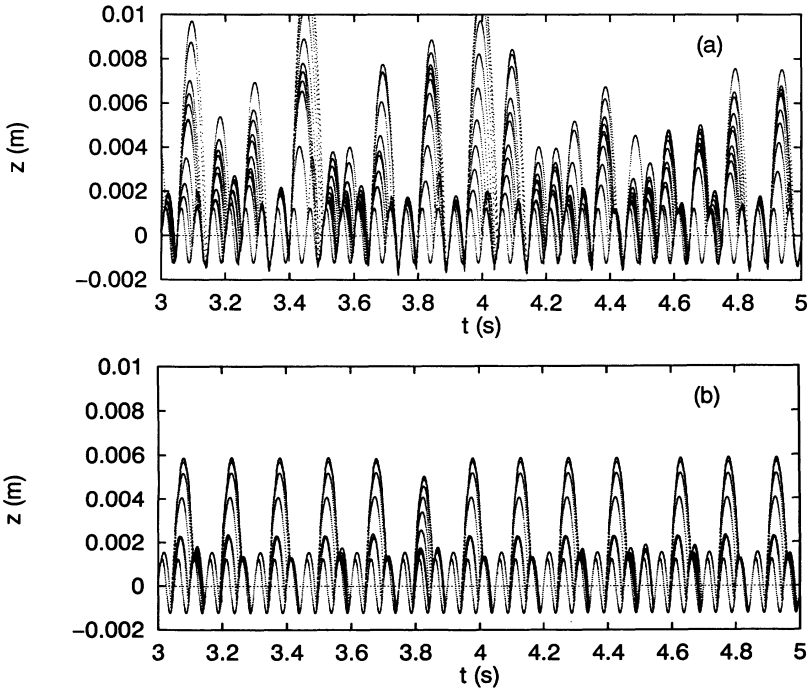

FIG. 5. Plotted are the MD trajectories (reduced z_i) of $N=10$ beads with $\varepsilon=0.6$ for $A_0=1.24d$ and $f=20$ Hz. The contact times are $t_c=0.7\times 10^{-3}$ s (a) and $t_c=0.7\times 10^{-5}$ s (b).

the apparatus can be found in Refs. [38,39]. The experiment is monitored by a camera that *moves horizontally,* at a regular pace, in front of the cell. The display is lighted using a stroboscopic flashing light tuned to a frequency slightly different from the excitation frequency. In this way, we obtain a (false) slowing down impression. An image processing device hooked to the camera records and accumulates the traces of the beads' centers of mass. One thus observes the positions of the beads as a function of the phase of the excitation. In Fig. 6(a) we show such a picture for an acceleration of $\alpha=2$ and a frequency of $f=10$ Hz. The column appears to stay clustered in all cases considered by us. In Fig. 6(b) we present a MD simulation for the trajectory of the centers of mass of the beads for the same parameters. The MD calculation may lead to large separations in the positions of the beads. On the other side an ED algorithm leads to clustered dynamics.

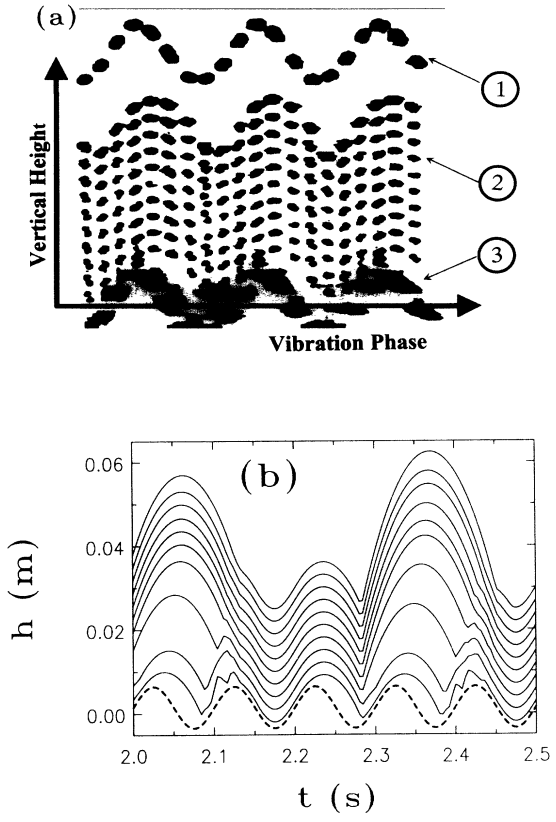

FIG. 6. (a) Experimental result of a 1D column of $N=10$ aluminum beads under vibration with $f=10$ Hz, and $\alpha=2$. Plotted is the vertical position as a function of the vibration phase. ① indicates the position of a reference bead, glued some 14 bead diameters above the bottom plate. ② indicates the position of the center of mass (dark dot) of the seventh bead. ③ indicates the bottom plate. (b) Results of MD simulations under the same conditions as in (a). The trajectories of the particles are represented as a function of time. The parameters used are $\varepsilon=0.6$ and $t_c=3.6\times10^{-6}$ s.

C. The behavior of a column of beads under strong agitation

We now turn to the question of strong agitation. This will lead to a large separation between the particles, $\sigma\gg1$, which means large dilatation and a long time of free flight s_0/v_0 between the collisions. This allows us to choose quite long contact times as long as $\sigma\gg1$. So the simulations should lead to comparable results in the high-energy and low-dissipation regime (HLR). The computer time needed for event-driven algorithms is proportional to the number of events; these algorithms are therefore most effective in HLR. MD algorithms consume computer time proportionally to the simulated time and are therefore less effective in HLR. Furthermore, the detachment effect will be strongest in the low-energy high-dissipation regime, because there the particles are almost always in contact.

In Ref. [39] a scaling behavior for the center of mass $h_{\text{c.m.}}$ was found in the case of high agitation α, low dissipation $(1-\varepsilon)\ll1$, and large number of particles N [i.e., $N(1-\varepsilon)<2.8$]:

$$h_{\text{c.m.}}=h_{\text{c.m.0}}+\frac{4}{3}\frac{(A_0\omega)^2}{g}\frac{\varphi(X)}{X}\ , \tag{10a}$$

where $h_{\text{c.m.0}}$ is the height of the center of mass at rest, X is the effective dissipation $X=N(1-\varepsilon)$, and $\varphi(X)$ is defined through

$$\varphi(X)=1-a_1X-a_2X^2\ , \tag{10b}$$

with $a_1=0.098$ and $a_2=0.073$. In Fig. 7 we display results of ED and MD simulations of $N=10$ particles with $\varepsilon=0.92$ and $f=20$ Hz. In Fig. 7 the crosses denote the ED and the circles denote the MD results. Furthermore we compare the results with Eq. (10a), depicted as a dashed line. Note that we are here in the regime of strong agitation so that we find $\sigma>10$, much larger than unity. In fact, in such a situation our requirement that t_c be close to its experimental value is no longer stringent and can be relaxed. The MD values in Fig. 7 were obtained with $t_c\cong10^{-4}$ s by averaging $h_{\text{c.m.}}$ over more than

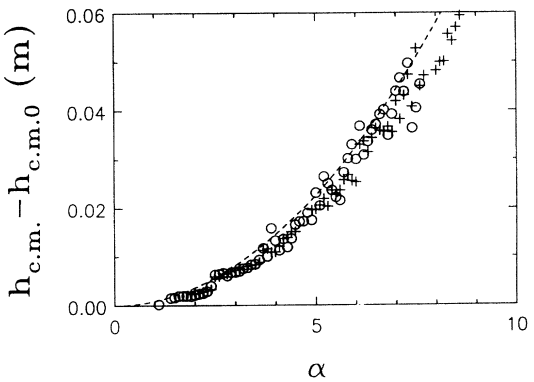

FIG. 7. Behavior of a 1D column of $N=10$ particles with $\varepsilon=0.92$ under vibration with $f=20$ Hz, and varying amplitude. We compare the MD (circles) with the ED simulations (crosses) and with the expression Eq. (10) (dashed line). Here α is the reduced acceleration $\alpha=A_0\omega^2/g$.

100 periods. In fact, using smaller t_c does not change the picture. As a result we find that for $\sigma \gg 1$ the MD methods reflect in a reliable way the ED and experimental results without having to require extensive computation.

The above simulations in 1D show that when the acceleration is high and the dissipation is low both the MD and the ED results are reliable. Problems with the simple MD simulations with large t_c become apparent when the dissipation (or the number of dissipative contacts) gets high and the acceleration α gets to be low. Then it is imperative to get to lower t_c values, by a judicious choice of the interaction parameters; the price to be paid is longer computation times.

VI. CONCLUSIONS

In this paper we have shown that MD simulations based on linear interactions and which use parameters which lead to large contact times t_c run into problems when they are used to determine the behavior of dense packings of beads. When the number of dissipative contacts is large, the MD calculations imply a too-low energy dissipation in the system considered. This means that the MD simulations overestimate the density and energy fluctuations. The effect is most obvious for linear interaction laws but also subsists for nonlinear interaction laws. As a measure for the occurrence of such effects, one can use the ratio σ between the time of free-flight and the contact time t_c. For $\sigma \ll 1$ the MD simulations underestimate the energy dissipation and lead to large fluctuations. Such computation-induced phenomena can be inhibited by using physically reasonable, small values for the time t_c. As will be shown by us elsewhere [42], such t_c values often suppress much of the convection shown in MD calculations; hence we infer that convection may be a spurious effect. On the other hand, for $\sigma \gg 1$ no particular precautions are necessary and we find that the results of MD and ED simulations agree with each other. Evidently, more work is necessary in order to determine optimal parameters for MD simulations. For the study of effects such as heaping, size segregation, and convection one may have to include, besides reasonable contact times, also the static friction and the rotation of the particles. For the microscopic interactions, possibly aspects like memory (hysteresis) may be important [47,48]. Maybe even the idea of pairwise interactions must be reconsidered in situations when, as a rule, a particle is in contact with several of its neighbors.

ACKNOWLEDGMENTS

LAOMC is a U.R.A. of the CNRS and this work was supported by a special grant A.T.P. "Matière en grain." We thank C. S. Campbell and Y-h. Taguchi for helpful discussions and H. J. Herrmann for the prototype source code of MD simulation. The support of the Deutsche Forschungsgemeinschaft (SFB 60), of the Fonds der Chemischen Industrie, and of the PROCOPE scientific collaboration program is acknowledged.

APPENDIX

In the following we consider nonlinear interactions between particles. Using Eq. (8) we present estimates for the contact time t_c, the maximal penetration $x_{\max}$, and the coefficient of restitution ε.

The elastic energy is $E_{\rm el}=Ed^{1-\beta}x_{\max}^{2+\beta}/(2+\beta)$, as can be found by setting $\eta=0$ in Eq. (8) and integrating it in standard fashion, after multiplication by $\dot{x}$. Here $x_{\max}$ is the maximal depth of penetration. Suppose that the initial kinetic energy $E_k=mv_0^2/2$ is completely transferred to elastic energy. This leads to a maximal penetration depth of

$$x_{\max}=\left[1+\frac{\beta}{2}\right]^{1/(2+\beta)}\left[\frac{m}{Ed^{1-\beta}}\right]^{1/(2+\beta)}(v_0)^{2/(2+\beta)} . \tag{A1}$$

Separating the energy conservation equation into t- and x-dependent terms and integrating from $t=0$ to $t_c/2$ or from $x=0$ to $x_{\max}$ the contact time t_c follows:

$$\begin{aligned} t_c &= I(\beta)\frac{x_{\max}}{v_0} \\ &= I(\beta)\left[1+\frac{\beta}{2}\right]^{1/(2+\beta)}\left[\frac{m}{Ed^{1-\beta}}\right]^{1/(2+\beta)} \\ &\quad\times(v_0)^{-\beta/(2+\beta)} . \end{aligned} \tag{A2}$$

In Eq. (A2) $I(\beta)$ is

$$I(\beta)=\frac{\sqrt{\pi}\,\Gamma\left[\frac{1}{2+\beta}\right]}{(1+\beta/2)\Gamma\left[\frac{4+\beta}{4+2\beta}\right]}=\begin{cases}\pi & \text{for } \beta=0\\ 2.94 & \text{for } \beta=\frac{1}{2}\end{cases},$$

where $\Gamma(z)$ is the gamma function. From Eq. (A2) one infers that the contact time follows $t_c \propto v_0^{-1/5}$ for the Hertz interaction law ($\beta=\frac{1}{2}$); Eqs. (A1) and (A2) lead to the expressions of Ref. [44], valid for two spherical particles, when one sets $E=Y/[3(1-\tilde{\sigma}^2)]$; here Y is the Young modulus and $\tilde{\sigma}$ the Poisson ratio. We tested, using the MD formalism for binary collisions, that $x_{\max}$ and t_c obey the above Eqs. (A1) and (A2) within 0.1%, as long as the dissipation is weak (i.e., $\varepsilon>0.9$). One test consists of simulating the pairwise collisions of 200 particles, while varying the initial relative velocity v_0 of each pair. This leads to a set of data that agrees with Eqs. (A1) and (A2) over more than 15 orders of magnitude in v_0.

Now we approximate the dissipated energy (in the weakly dissipative regime) through

$$E_{\rm diss} \propto F_{\rm diss}x_{\max} \propto (\eta d^{1-\gamma}v_0)x_{\max}^{1+\gamma} ,$$

which leads to

$$\begin{aligned} E_{\rm diss} &\propto \eta d^{1-\gamma}\left[\frac{m}{Ed^{1-\beta}}\right]^{(1+\gamma)/(2+\beta)} \\ &\quad\times v_0^{(2+\gamma+\beta/2)/(1+\beta/2)} . \end{aligned} \tag{A3}$$

For a loss coefficient $1-\varepsilon \propto 1-\sqrt{1-E_{\rm diss}/E_0}$ we obtain

$$1-\varepsilon \propto v_0^{(2\gamma-\beta)/(2+\beta)} . \tag{A4}$$

For the Hertz-Kuwabara-Kono model ($\beta=\gamma=\frac{1}{2}$), one finds a *slow* increase of $1-\varepsilon$ with the velocity, i.e., $1-\varepsilon \propto v_0^{1/5}$. Note also the behavior in the case $\beta=\frac{1}{2}$ and $\gamma=0$ for it was considered in Refs. [28,29] one finds $1-\varepsilon \propto v_0^{-1/5}$, i.e., beads are more elastic at higher velocities. We suggest that this might be one reason why no steady state for a system of particles on an inclined chute is found [28]. Due to gravity the particles are accelerated; if there is less dissipation at higher velocities, there is no reason for a steady state to build up. On the other hand, if the dissipation increases with the velocity one has two effects which balance each other. In Table I we summarize the findings and give the corresponding references. Note that the penetration depth and the contact time depend only on β, while the behavior of $1-\varepsilon$ can be varied by changing the exponent γ. Most nonlinear MD simulations [28–30,32] were carried out using $\gamma=0$; this means that $1-\varepsilon$ is proportional to $v_0^{-1/5}$ (i.e., at higher velocity one has less dissipation).

TABLE I. The exponents ν_1, ν_2, and ν_3, which give the v_0 dependence of $x_{\max} \propto v_0^{\nu_1}$, $t_c \propto v_0^{\nu_2}$, and $1-\varepsilon \propto v_0^{\nu_3}$ in the limit of low dissipation (η small). The interaction law is Eq. (8) of the main text.

β	γ	ν_1	ν_2	ν_3	Refs.
0	0	1	0	0	[24–27]
0	$\frac{1}{5}$	1	0	$\frac{1}{5}$	
$\frac{1}{2}$	0	$\frac{4}{5}$	$-\frac{1}{5}$	$-\frac{1}{5}$	[28–30,32]
$\frac{1}{2}$	$\frac{1}{2}$	$\frac{4}{5}$	$-\frac{1}{5}$	$\frac{1}{5}$	[43]
$\frac{1}{2}$	$\frac{1}{4}$	$\frac{4}{5}$	$-\frac{1}{5}$	0	[45]

[1] R. L. Brown and J. C. Richard, *Principle of Powder Mechanics* (Pergamon Press, Oxford, 1966).
[2] H. M. Jaeger and S. R. Nagel, Science **255**, 1523 (1992).
[3] S. Savage, J. Fluid, Mech. **194**, 457 (1988).
[4] P. Evesque and J. Rajchenbach, Phys. Rev. Lett. **61**, 44 (1989).
[5] S. Douady, S. Fauve, and C. Laroche, Europhys. Lett. **8**, 621 (1989).
[6] E. Clément and J. Rajchenbach, Europhys. Lett. **16**, 149 (1991).
[7] E. Clément, J. Duran, and J. Rajchenbach, Phys. Rev. Lett. **69**, 1189 (1992).
[8] H. K. Pak and P. P. Behringer, Phys. Rev. Lett. **71**, 1832 (1993).
[9] J. C. Williams, Powder Technol. **15**, 245 (1976).
[10] J. B. Knight, H. M. Jaeger, and S. R. Nagel, Phys. Rev. Lett. **70**, 3728 (1993).
[11] J. Duran, J. Rajchenbach, and E. Clément, Phys. Rev. Lett. **70**, 2431 (1993).
[12] A. Suzuki, H. Takahashi, and T. Tanaka, Powder Technol. **2**, 72 (1968).
[13] A. Rosato and Y. Lan, in *Powders and Grains 93,* edited by C. Thornton (Balkema, Rotterdam, 1993), p. 241.
[14] C. Brennen, S. Gosh, and Wassgren, in *Powders and Grains 93,* edited by C. Thornton (Balkema, Rotterdam, 1993), p. 247.
[15] C-h. Liu and S. R. Nagel, Phys. Rev. Lett. **68**, 2301 (1992).
[16] S. B. Savage, J. Fluid Mech. **92**, 53 (1979).
[17] S. B. Savage, in *Disorder and Granular Media,* edited by D. Bideau (North-Holland, Amsterdam, 1993).
[18] P. C. Johnson and R. Jackson, J. Fluid. Mech. **176**, 67 (1987).
[19] S. F. Edwards and R. B. S. Oakeshott, Physica A **157**, 1080 (1989).
[20] M. W. Richman, Mech. Mater. **16**, 211 (1993).
[21] M. P. Allen and D. J. Tildesley, *Computer Simulation of Liquids* (Oxford University Press, Oxford, 1987).
[22] P. A. Cundall and O. D. L. Strack, Geotechnique **29**, 47 (1979).
[23] P. A. Thompson and G. S. Grest, Phys. Rev. Lett. **67**, 1751 (1990).
[24] Yi Zhang and C. S. Campbell, J. Fluid Mech. **237**, 541 (1992).
[25] Y-h. Taguchi, Phys. Rev. Lett. **69**, 1367 (1992).
[26] Y-h. Taguchi, Int. J. Mod. Phys. B **7**, 1839 (1993).
[27] J. A. C. Gallas, H. J. Herrmann, and S. Sokolowski, Phys. Rev. Lett. **69**, 1371 (1992).
[28] T. Pöschel, J. Phys. II **3**, 27 (1993).
[29] G. H. Ristow, Int. J. Mod. Phys. C **3**, 1281 (1992).
[30] J. Lee and H. J. Herrmann, J. Phys. A **26**, 373 (1993).
[31] J. Lee, J. Phys. (Paris) I **3**, 2017 (1993).
[32] J. Lee, J. Phys. A **27**, L257 (1994).
[33] S. McNamara and W. R. Young, Phys. Fluids A **4**, 496 (1992).
[34] S. McNamara and W. R. Young, Phys. Fluids A **5**, 34 (1993).
[35] B. Bernu and R. Mazighi, J. Phys. A **23**, 5745 (1990).
[36] B. Bernu, F. Delyon, and R. Mazighi, Phys. Rev. E (to be published).
[37] B. D. Lubachevsky, J. Comput. Phys. **94**, 255 (1991).
[38] E. Clément, S. Luding, A. Blumen, J. Rajchenbach, and J. Duran, Int. J. Mod. Phys. B **7**, 1807 (1993).
[39] S. Luding, E. Clément, A. Blumen, J. Rajchenbach, and J. Duran, Phys. Rev. E **49**, 1634 (1994).
[40] S. F. Foerster, M. Y. Louge, H. Chang, and K. Allia, Phys. Fluids **6**, 1108 (1994).
[41] J. Duran, T. Mazozi, E. Clément, and J. Rajchenbach, Phys. Rev. E **50**, 1762 (1994).
[42] S. Luding, E. Clément, A. Blumen, J. Rajchenbach, and J. Duran, Phys. Rev. E **50**, 1762 (1994).
[43] G. Kuwabara and K. Kono, Jpn. J. Appl. Phys. **26**, 1230 (1987).
[44] L. D. Landau and E. M. Lifschitz, *Band VII Elastizitätstheorie* (Akademie Verlag, Berlin, 1989), Exercise 1 of Sec. 9.
[45] Y-h. Taguchi, J. Phys. (Paris) II **2**, 2103 (1992).
[46] A. Mehta and J. M. Luck, Phys. Rev. Lett. **65**, 393 (1990).
[47] M. H. Sadd. Q. Tai, and A. Shukla, Int. J. Non-Linear Mech. **28**, 251 (1993).
[48] O. R. Walton and R. L. Braun, Acta Mech. **63**, 73 (1986).

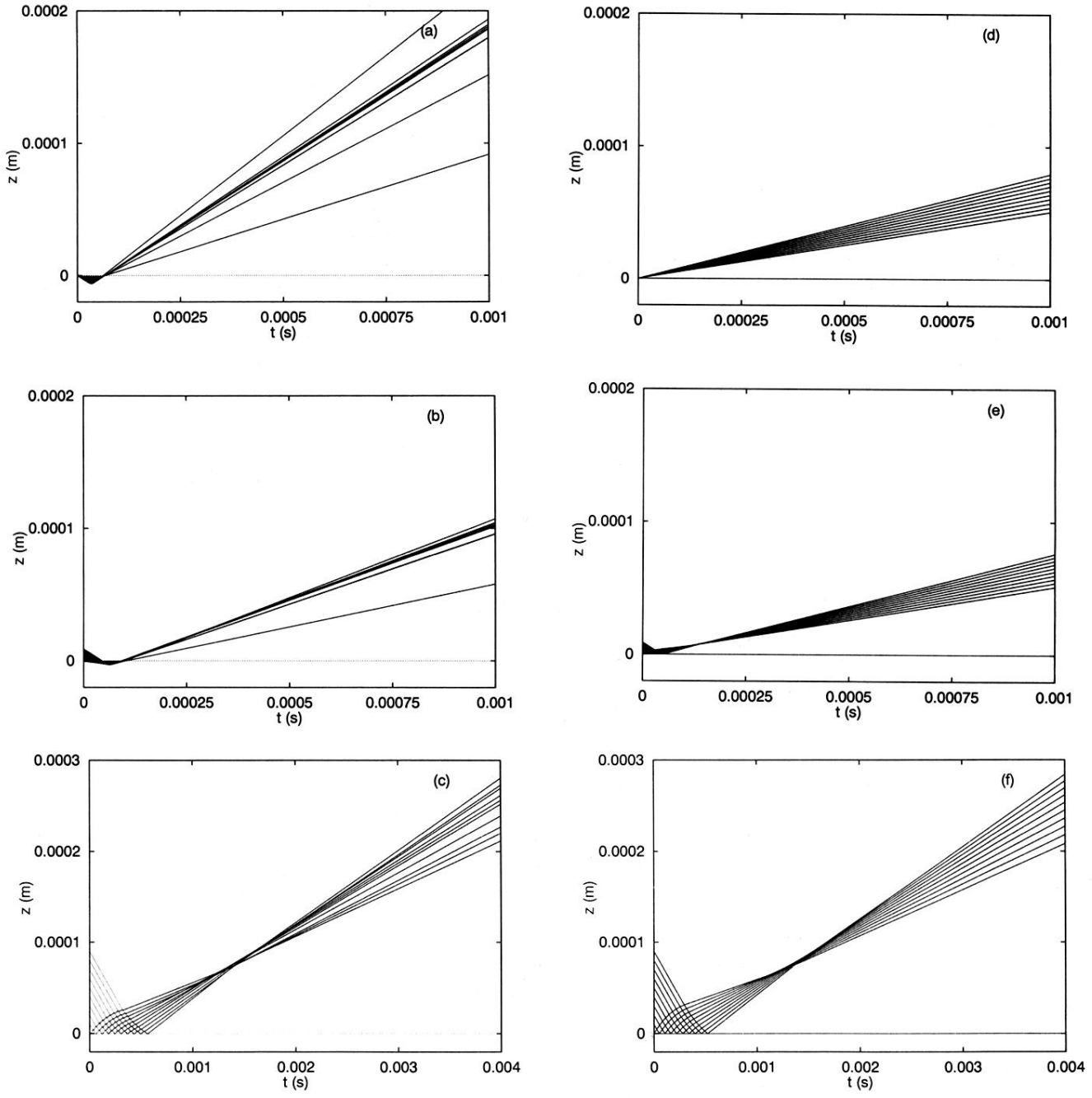

FIG. 1. (a) MD trajectories of the centers of $N=10$ particles which collide with a fixed boundary. Here $\varepsilon=0.9$, $t_c=0.7\times10^{-5}$ s, $v_0=-0.2$ m/s, and $s_0=0$ m. The positions are in reduced units, Eq. (9). (b) The same as in (a) but with $s_0=10^{-6}$ m. (c) The same as in (a) but with $s_0=10^{-5}$ m. Note the different axes. (d) ED trajectories of the centers of $N=10$ particles; the parameters are as in (a); especially $s_0=0$ m. (e) The same as in (d) but with $s_0=10^{-6}$ m. (f) The same as in (d) but with $s_0=10^{-5}$ m. Note the different axes.

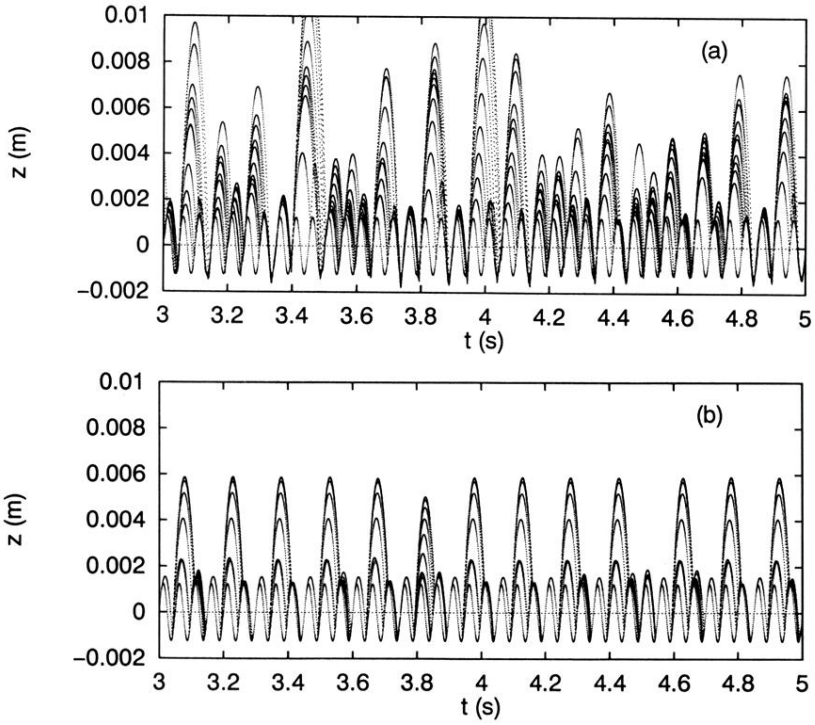

FIG. 5. Plotted are the MD trajectories (reduced z_i) of $N=10$ beads with $\varepsilon=0.6$ for $A_0=1.24d$ and $f=20$ Hz. The contact times are $t_c=0.7\times10^{-3}$ s (a) and $t_c=0.7\times10^{-5}$ s (b).